656 *Inorg. Chem.* **1997,** *36,* 656−660

Solid State and Solution Study of Trinuclear (Ni, Ba, Ni) Complexes: $(L^1{}_2Ni)_2Ba(ClO_4)_2\cdot 2H_2O$ (1) and $(L^2{}_2Ni)_2Ba(ClO_4)_2\cdot 2H_2O$ (2) (L^1 = 3-Methoxysalicylaldiminato and L^2 = 3-(2-Methoxyethoxy)salicylaldiminato). Crystal and Molecular Structure of 2

Jean-Pierre Costes,* Jean-Pierre Laurent, Philippe Chabert, Gérard Commenges, and Françoise Dahan

Laboratoire de Chimie de Coordination du CNRS, UPR 8241, liée par conventions à l'Université Paul
Sabatier et à l'Institut National Polytechnique de Toulouse, 205 route de Narbonne,
31077 Toulouse Cedex, France

Received July 18, 1996[⊗]

The nickel(II) complexes of L^1 = 3-methoxysalicylaldiminato and L^2 = 3-(2-methoxyethoxy)salicylaldiminato react with barium ions to afford bimetallic complexes characterized by a Ba to Ni ratio of 1/2. A structural determination of the complex $(L^2{}_2Ni)_2Ba(ClO_4)_2\cdot 2H_2O$ (**2**) shows that it crystallizes in the orthorhombic space group *Pbca* (No. 61) with 8 formula units in the cell having the dimensions $a = 14.780(1)$ Å, $b = 24.888(2)$ Å, and $c = 27.291(2)$ Å. In the presence of barium ions, the precursor complexes $L^1{}_2Ni$ and $L^2{}_2Ni$ change their configurations from trans to cis so as to offer a polyoxygenated coordination site to a barium ion and assemble themselves around that ion to yield bimetallic species. Structural analogies with the polyether complexes of barium are discussed. Solution studies point to a great sensitivity of **2** to the nature of the solvent, contrary to $(L^1{}_2Ni)_2Ba(ClO_4)_2\cdot 2H_2O$ (**1**). Indeed, an important dissociation is induced by solvents which display good donor properties and which are able to stabilize the barium ions via solvation.

Introduction

It has been shown that the nickel(II) complexes of 3-methoxysalicylaldiminato and related compounds with polyether side arms are able to add alkali metal cations.[1−9] To date, three types of bimetallic (Ni, Na) complexes have been structurally characterized. Addition of sodium picrate to the L_2Ni (L = 3-methoxy-*N*-methylsalicylaldiminato) precursor leads to a paramagnetic species, $(L_2NiNaX)_2\cdot H_2O$ (X standing for the picrate ion), which displays an unexpected cage structure with two side arms used to bind Na^+, another to bind Ni^{2+}, and a fourth free-standing functionality.[3,6] However diamagnetic complexes with simpler structures (**3** and **4** in Figure 1) have been obtained from the reaction of $Na^+$with $L^1{}_2Ni$ and $L^2{}_2Ni$, respectively (L^1 stands for 3-methoxysalicylaldiminato and L^2 for 3-(2-methoxyethoxy)salicylaldiminato. Structural studies show that, in both cases, the monometallic precursor $L^1{}_2Ni$ or $L^2{}_2Ni$ reacts with Na^+ to yield a bimetallic (Ni, Na) species which has an inner cis N_2O_2Ni chromophore and can accommodate Na^+ in the ether-like outer cavity.[8,9] In order to specify the ability of the monometallic precursors to mimic aliphatic or crown ethers, we have investigated the products of their reaction with barium ions.

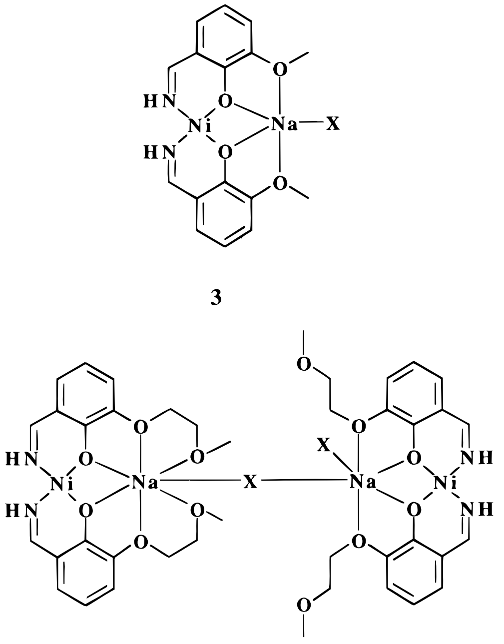

3

4

Figure 1. Schematic representation of the complexes $L^1{}_2NiNaX$ (**3**) and $[L^2{}_2NiNaX]_2$ (**4**). In both cases X stands for ClO_4.

Experimental Section

Elemental analyses were carried out by the Service de Microanalyse du Laboratoire de Chimie de Coordination, Toulouse, France (C, H, N). Electronic spectra were obtained with a Cary 2300 spectrometer, using acetone or dmso as solvent. 1D ^1H NMR spectra were acquired at 250.13 MHz on a Bruker WM250 spectrometer. 1D ^{13}C spectra using ^1H broad-band decoupling, $\{^1H\}^{13}C$, and gated ^1H decoupling with selective proton irradiation during acquisition were obtained with the Bruker WM250 apparatus working at 62.89 MHz. Variable-

---

[⊗] Abstract published in *Advance ACS Abstracts,* January 15, 1997.

(1) van Staveren, C. J.; van Eerden, J.; van Veggel, F. C. J. M.; Harkema, S.; Reinhoudt, D. N. *J. Am. Chem. Soc.* **1988**, *110*, 4994.
(2) Lindsey, J. S. *New. J. Chem.* **1991**, *15*, 153.
(3) Schall, O. F.; Robinson, K.; Atwood, J. L.; Gokel, G. W. *J. Am. Chem. Soc.* **1993**, *115*, 5962.
(4) Lehn, J. M. *Angew. Chem., Int. Ed. Engl.* **1990**, *29*, 1304.
(5) Schepartz, A.; McDevitt, J. P. *J. Am. Chem. Soc.* **1989**, *111*, 5976.
(6) Schall, O. F.; Robinson, K.; Atwood, J. L.; Gokel, G. W. *J. Am. Chem. Soc.* **1991**, *113*, 7434.
(7) Jones, M. W.; Gupta, N.; Schepartz, A.; Thorp, H. H. *Inorg. Chem.* **1992**, *31*, 1308.
(8) Costes, J. P.; Dahan, F.; Laurent, J. P. *Inorg. Chem.* **1994**, *33*, 2738.
(9) Costes, J. P.; Dahan, F.; Laurent, J. P. *Inorg. Chem.* **1995**, *34*, 3102.

S0020-1669(96)00856-7 CCC: $14.00

temperature recordings, 2D ^{1}H COSY experiments using standard programs, and 2D pulse-field gradient HMQC ^{1}H−^{13}C correlation using the PFG-HMQC standard program were performed on a Bruker AMX400 spectrometer. Chemical shifts are given in ppm *versus* TMS (^{1}H and ^{13}C) using CD_2Cl_2, CD_3COCD_3, or $(CD_3)_2SO$ as solvent. Positive fast atom bombardment (FAB) mass spectra were recorded by means of a NERMAG R10-10 spectrometer with the samples introduced in a *m*-nitrobenzyl alcohol matrix. Cryometric measurements were performed in $(CH_3)_2SO$ at concentrations of ca. 1.5 × 10^{-2} M.

Caution. The complexes reported here were isolated as perchlorate salts. We worked with these complexes in a number of organic solvents without any incident, and as solids, they seem to be reasonably stable to shock and heat. In spite of these observations, the unpredictable behavior of perchlorate salts[10] necessitates extreme care in their handling.

Materials. All starting materials were purchased from Aldrich and were used without further purification. 3-(2-Methoxyethoxy)-*p*-toluenesulfonate[11] and 3-(2-methoxyethoxy)salicylaldehyde[3] were prepared according published procedures. Preparation of the complexes $L^1{}_2NiNaClO_4$ (**3**), $L^2{}_2NiNaClO_4$ (**4**), $L^1{}_2Ni.2H_2O$, and $L^2{}_2Ni$ along with the FAB data and some NMR results were given in previous papers.[8,9] New results are reported herein.

$L^2{}_2$Ni. ^{1}H NMR (250 MHz, 20 °C, $(CD_3)_2CO$): δ 3.496 (s, CH_3), 3.739 (b, CH_2OCH_3), 4.150 (b, CH_2OAr), 6.550 (t, J = 7.8 Hz, Ar CH(5)), 6.949 (d, J = 7.8 Hz, Ar CH(4)), 7.091 (d, J = 7.8 Hz, Ar CH(6)), 7.948 (d, J = 11.3 Hz, HC═N), 8.355 (b, C═NH). ^{1}H NMR (250 MHz, 20 °C, $(CD_3)_2SO$): δ 3.426 (s, CH_3), 3.710 (t, J = 4.6 Hz, CH_2OCH_3), 4.125 (t, J = 4.6 Hz, CH_2OAr), 6.533 (t, J = 7.9 Hz, ArCH(5)), 6.923 (dd, J = 7.9 and 1.5 Hz, ArCH(4)), 7.099 (dd, J = 7.9 and 1.5 Hz, ArCH(6)), 7.945 (d, J = 11.8 Hz, HC═N), 8.409 (d, J = 11.8 Hz, C═NH).

Complex 1: $(L^1{}_2Ni)_2Ba(ClO_4)_2\cdot 2H_2O$. $L^1{}_2Ni\cdot 2H_2O$[8] (0.3 g, 7.6 10^{-4} mol) was partly dissolved in acetone (20 mL). Addition of a slight excess of barium perchlorate (0.29 g, 8.6 10^{-4} mol) to the stirred solution yielded the desired product, which precipitated a few minutes later. The precipitate was filtered off, washed with acetone and diethyl ether, and dried (0.63 g, 74% yield).

Anal. Calcd for $C_{32}H_{36}BaCl_2N_4Ni_2O_{18}$: C, 35.2; H, 3.3; N, 5.1. Found: C, 34.9; H, 3.4; N, 4.9. Mass spectrum (FAB, 3-nitrobenzyl alcohol matrix)), *m/z*: 945 (11), $[C_{32}H_{32}BaClN_4Ni_2O_{12}]^+$; 846 (3.8), $[C_{32}H_{32}BaN_4Ni_2O_8]^+$; 587 (100), $[C_{16}H_{16}BaClN_2NiO_8]^+$. UV−vis, nm: (solid) 570, 395; (acetone) 540, 395; (dmso) 545, 405. Electrical conductivity: $\Lambda = 256\ \Omega^{-1}\ m^2\ equiv^{-1}$. Cryoscopy: experimental, 309; theoretical, 1090; theo/exp = 3.5. ^{1}H NMR (250 MHz, 20 °C, $(CD_3)_2CO$): δ 2.984 (s, H_2O), 3.814 (s, CH_3), 6.707 (t, J = 7.9 Hz, ArCH(5)), 6.855 (d, J = 7.9 Hz, ArCH(4)), 7.117 (d, J = 7.9 Hz, ArCH(6)), 8.900 (b, HC═N + C═NH). ^{1}H NMR (250 MHz, 20 °C, $(CD_3)_2SO$): δ 3.468 (s, 8H, H_2O), 3.717 (s, CH_3), 3.804 (s, CH_3), 6.563 (b, ArCH(5)), 6.692 (b, ArCH(5)), 6.871 (b, ArCH(4)), 7.072 (b, ArCH(6)), 7.924 (b, HC═N), 8.332 (b, HC═N + C═NH), 8.489 (b, C═NH). $^{13}C\{^1H\}$ NMR (62.89 MHz, 20 °C, $(CD_3)_2SO$): δ 55.85 (CH_3), 114.24 (Ar C(5)H), 115.65 (Ar C(4)H), 120.56 (Ar C(1)), 125.24 (Ar C(6)H), 151.20 (Ar C(2)), 166.94 (HC═N).

Complex 2: $(L^2{}_2Ni)_2Ba(ClO_4)_2\cdot 2H_2O$. A similar procedure[9] using $L^2{}_2Ni$ (0.3 g, 6.7 10^{-4} mol) and methanol instead of $L^1{}_2Ni$ and acetone yielded complex **2**, which precipitated from the solution and was filtered off, washed with cold methanol and diethyl ether, and dried (0.60 g, 70% yield).

Anal. Calcd for $C_{40}H_{52}BaCl_2N_4Ni_2O_{22}$: C, 37.9; H, 4.1; N,4.4. Found: C, 37.5; H, 4.0; N, 4.3. Mass spectrum (FAB, 3-nitrobenzyl alcohol matrix)), *m/z*: 675 (100), $[C_{20}H_{24}BaClN_2NiO_{10}]^+$; 576 (41.0), $[C_{20}H_{24}BaN_2NiO_6]^+$. UV−vis, nm: (solid) 580, 395; (acetone) 545, 395; (dmso) 555, 410. Electrical conductivity: $\Lambda = 266\ \Omega^{-1}\ m^2\ equiv^{-1}$. Cryoscopy: experimental, 219; theoretical, 1266; theo/exp = 5.8. ^{1}H NMR (250 MHz, 20 °C, CD_2Cl_2): δ 3.759 (s, CH_3), 4.192(b, CH_2OCH_3), 4.483 (b, CH_2OAr), 6.834 (m, b, ArCH(5)), 7.245 (m, b, ArCH(4+6)), 8.068 (b, HC═N + C═NH). ^{1}H NMR (400 MHz, 20 °C, $(CD_3)_2CO$): δ 3.055 (s, H_2O), 3.724 (a′) (s, CH_3), 3.758 (a) (s, CH_3), 3.879 (c′) (b, CH_2OCH_3), 4.185 (c) (b, CH_2OCH_3), 4.268 (b′) (b, CH_2OAr), 4.483 (b) (b, CH_2OAr), 6.798 (m, b, ArCH(5)), 6.945 (m, b, ArCH(5)), 7.328 (m, b, ArCH(4+6)), 7.374 (m, b, ArCH(4+6)), 7.927 (b, HC═N + C═NH), 8.231 (b, HC═N + C═NH). ^{1}H NMR (400 MHz, −60 °C, $(CD_3)_2CO$): δ 3.682 (s, 4H, H_2O), 3.732 (a′) (s, CH_3), 3.744 (a) (s, CH_3), 3.803 (e′) (b, CH_2OCH_3), 3.831 (f′) (b, CH_2OCH_3), 4.118 (f) (b, CH_2OAr), 4.146 (e) (b, CH_2OAr), 4.224 (c) (b, CH_2OCH_3), 4.429 (b) (b, CH_2OAr), 6.735 (t, J = 7.9 Hz, ArCH(5)), 6.877 (t, J = 7.9 Hz, ArCH(5)), 7.283 (m, ArCH(4+6)), 7.841 (d, J = 11.4 Hz, C═NH), 7.897 (d, J = 11.4 Hz, HC═N), 8.165 (d, J = 11.4 Hz, HC═N), 8.278 (d, J = 11.4 Hz, C═NH). ^{1}H NMR (250 MHz, 20 °C, $(CD_3)_2SO$): δ 3.473 (s, H_2O), 3.443 (s, CH_3), 3.753 (b, CH_2OCH_3), 4.164 (b, CH_2OAr), 6.610 (b, ArCH(5)), 6.968 + 7.121 (b, ArCH(4+6), 7.942 (b, HC═N), 8.438 (b, C═NH). $^{13}C\{^1H\}$ NMR (62.89 MHz, 20 °C, $(CD_3)_2CO$): δ 58.71, 59.25 (CH_3), 67.52 (CH_2), 69.94, 70.24, 70.28 (CH_2), 116.07 (Ar C(5)H), 116.58, 119.92 (Ar C(4)H), 120.82, 121.73 (Ar C(1)), 126.92, 127.84 (Ar C(6)H), 148.28 (Ar C(3)), 151.94 (Ar C(2)), 167.78, 168.56 (HC═N). $^{13}C\{^1H\}$ NMR (62.89 MHz, 20 °C, $(CD_3)_2SO$): δ 58.29 (CH_3), 67.33 (b, CH_2), 69.79 (b, CH_2), 115.60 (b, Ar C(5)H), 116.76 (b, Ar C(4)H), 121.27 (Ar C(1)), 126.00 (Ar C(6)H), 153.21 (b, Ar C(2)), 168.45 (b, HC═N). ^{1}H NMR of **2** + $Ba(ClO_4)_2$ (250 MHz, 20 °C, $(CD_3)_2CO$): δ 3.212 (s, H_2O), 3.762 (s, CH_3), 4.185 (t, J = 4.4 Hz, CH_2OCH_3), 4.488 (t, J = 4.4 Hz, CH_2OAr), 6.836 (t, J = 7.7 Hz, ArCH(5)), 7.261 (dd, J = 7.7 and 0.5 Hz, ArCH(4+6)), 8.080 (b, HC═N + C═NH). $^{13}C\{^1H\}$ NMR of **2** + $Ba(ClO_4)_2$ (62.89 MHz, 20 °C, $(CD_3)_2CO$): δ 58.70 (CH_3), 67.53 (CH_2), 70.18 (CH_2), 116.56 (Ar C(5)H), 116.58 (Ar C(4)H), 120.76 (Ar C(1)), 126.89 (Ar C(6)H), 148.86 (Ar C(3)), 151.94 (Ar C(2)), 168.44 (HC═N).

Table 1. Crystallographic Data for $(C_{20}H_{24}N_2 0_6Ni)_2Ba(ClO_4)_2\cdot 2H_2O$ (**2**)

empirical formula	$C_{40}H_{52}BaCl_2N_4Ni_2O_{22}$	λ, Å	0.710 73
fw	1266.5	Z	8
crystal system	orthorhombic	D_c, g cm^{-3}	1.676
space group	*Pbca* (No. 61)	T, K	293
a, Å	14.780(1)	μ mm^{-1}	1.67
b, Å	24.888(2)	R^a	0.032
c, Å	27.291(2)	$R_w{}^b$	0.042
V, Å^3	10039(1)		

^{a} $R = \sum||F_o| - |F_c||/\sum|F_o|$. ^{b} $R_w = [\sum w(|F_o| - |F_c|)^2/\sum wF_o{}^2]^{1/2}$.

Complex 3: $L^1{}_2NiNaClO_4$. ^{1}H NMR (250 MHz, 20 °C, $(CD_3)_2CO$): δ 4.042 (s, CH_3), 6.581 (t, J = 7.9 Hz, ArCH(5)), 6.916 (d, J = 7.9 Hz, ArCH(4)), 7.985 (dd, J = 7.9 and 1.5 Hz, ArCH(6)), 7.966 (d, J = 11.5 Hz, HC═N), 8.050 (b, C═NH). UV−vis, nm: (solid) 570, 395; (acetone) 540, 395; (dmso) 540, 400. Electrical conductivity: $\Lambda = 119\ \Omega^{-1}\ m^2\ equiv^{-1}$. Cryoscopy: experimental, 238; theoretical, 481.5; theo/exp = 2.0.

Complex 4: $L^2{}_2NiNaClO_4$. ^{1}H NMR (250 MHz, 20 °C, $(CD_3)_2SO$): δ 3.450 (s, 8H, H_2O), 3.439 (s, CH_3), 3.742 (t, J = 4.1 Hz, CH_2OCH_3), 4.202 (t, J = 4.1 Hz, CH_2OAr), 6.635 (t, J = 7.2 Hz, ArCH(5)), 7.072 (d, J = 7.2 Hz, ArCH(4)), 7.134 (dd, ArCH(6)), 8.056 (d, J = 11.6 Hz, HC═N), 8.569 (d, J = 11.6 Hz, C═NH). UV−vis, nm: (solid) 580, 395; (acetone) 535, 400; (dmso) 535, 405. Electrical conductivity: $\Lambda = 122\ \Omega^{-1}\ m^2\ equiv^{-1}$. Cryoscopy: experimental, 277; theoretical, 569.5; theo/exp = 2.0.

X-ray Structure Determination. Data Collection and Processing. Crystal data are gathered in Table 1. Diffraction measurements were performed on an Enraf-Nonius CAD4 diffractometer.The unit-cell parameters were obtained from a least-squares fit of 25 reflections (with θ between 12.0 and 17.5°). Data were collected with the ω-2θ scan technique [scan width (0.70 + 0.35 tan θ)°; $2\theta_{max} = 52°$; $+h,+k,+l$) and a variable scan rate with a maximum scan time of 60 s per reflection. Lorentz and polarization corrections and empirical absorption corrections[12] from ψ scans ($T_{min-max}$ = 0.785−1.000) were applied using the MolEN package,[13] and the data were reduced to $|F_o|$ values.

---

[10] Everett, K.; Graf, F. A., Jr. In *CRC Handbook of Laboratory Safety*, 2nd ed.; Steere, N. V., Ed.; Chemical Rubber Co.: Cleveland, OH, 1971.

[11] Ouchi, M.; Inoue, Y.; Kanzaki, T.; Hakushi, T. *J. Org. Chem.* **1984**, *49*, 1408.

[12] North, A. C. T.; Phillips, D. C.; Mathews, F. S. *Acta Crystallogr., Sect. A* **1968**, *A21*, 351.

Three reflections measured every 2 h showed no significant intensity variations (±0.1%). A total of 9820 unique reflections were collected.

Structure Solution and Refinement. The structure was solved by Patterson techniques[14] and refined by full-matrix least-squares procedures.[15] The non-hydrogen atoms were refined anisotropically, except those of the phenyl rings, which were refined isotropically. The hydrogen atoms were included in calculated positions, each riding on the atom to which it is bonded, with isotropic thermal parameters kept fixed, except for those of hydrogens in the water molecules, which were allowed to vary. The final refinement cycle was based on 4248 observed reflections with $|F_o| > 5\sigma(|F_o|)$ and 532 variable parameters. The weighting scheme used was $w = [\sigma^2(F_o) + 0.0008F_o^2]^{-1}$. Final R and R_w values were 0.032 and 0.042. The maximum and minimum peaks on the final Fourier difference map corresponded to 0.32 and -0.31 e Å^{-3}, respectively. Neutral-atom scattering factors, including anomalous dispersion effects, were taken from the standard compilation.[16] All calculations were performed on a MicroVax 3400 computer, using the MolEN[13] package and SHELXS-86[14] and SHELX76[15] programs.

Results and Discussion

Structural determinations have shown that the nickel complexes L^1_2Ni and L^2_2Ni react with NaClO$_4$ to yield bimetallic species, L^1_2NiNaCLO$_4$ (**3**)[8] and [L^2_2NiNaClO$_4$]$_2$ (**4**),[9] in which the sodium is located in a crown ether like site. Similar reactions may be performed with Ba(ClO$_4$)$_2$, but the resulting products have a 1/2 Ba/Ni ratio. According to the elemental analysis data, they are well represented by the overall formulas $(L^1_2Ni)_2Ba(ClO_4)_2\cdot 2H_2O$ (**1**) and $(L^2_2Ni)_2Ba(ClO_4)_2\cdot 2H_2O$ (**2**), respectively. Inspection of the mass spectrum (FAB$^+$, *m*-nitrobenzyl alcohol) of **1** shows that the main signal ($I = 100\%$) occurs at $m/z = 587$[1] and, consequently, is attributable to $[(L^1_2Ni)Ba(ClO_4)]^+$. [In every case the correct ratios of the isotopes (C, Cl, Ni, Ba) are observed.] Peaks of lower intensities are observed at $m/z = 945$ ($I = 11\%$) and 846 ($I = 4\%$). They are attributable to $[(L^1_2Ni)_2Ba(ClO_4)]^+$ and $[(L^1_2Ni)_2Ba]^{2+}$, respectively. This behavior differs significantly from that observed for **3** and **4**,[8,9] where, in both cases, the most prominent signal corresponds to the species $[(L^i_2Ni)Na]^+$($m/z = 381$ and 469 for $i = 1$ and 2, respectively).[9] Surprisingly the FAB spectrum of **2** is even more different, since the peak corresponding to the species $[(L^2_2Ni)_2Ba(ClO_4)]^+$ is completely absent. Instead, one observes two groups of signals at $m/z = 675$ ($I = 100\%$) and 576 ($I = 40\%$). They are attributable to $[L^2_2NiBa(ClO_4)]^+$ and $[L^2_2NiBa]^{2+}$, respectively. These data suggest that in the barium complexes one of the L^i_2Ni groups is more labile than the other, this effect being very pronounced in the case of complex **2**.

Structure of Complex 2. The structure is represented in Figure 2,[17] and relevant bond lengths and angles are given in Table 2. The orthorhombic cell consists of eight complex cations $[(L^2_2Ni)_2Ba(H_2O)]^{2+}$, sixteen $(ClO_4)^-$ anions, and eight water molecules. With respect to the previously reported (Ni, Na) [8,9] complexes **3** and **4**, the most interesting feature of the title complex is that the Ba^{2+} ion is encapsulated between two $(L^2_2Ni)^x$ ($x = 1, 2$) units. It may be also noted that there is no short contact between Ba^{2+} and the perchlorate anions, while the perchlorates are integral parts of the structure of $[L^2_2NiNaClO_4]_2$.[9]

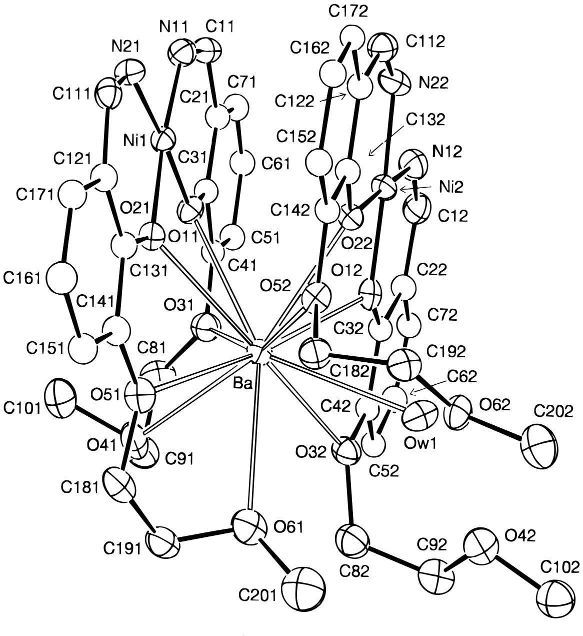

Figure 2. ORTEP plot for $(L^2_2Ni)_2Ba(ClO_4)_2\cdot 2H_2O$ (**2**) with ellipsoids drawn at the 30% probability level.

Table 2. Selected Bond Lengths (Å) and Angles (deg) with Esds in Parentheses for **2**

Ba−O(11)	2.796(4)	Ba−O(12)	2.777(4)
Ba−O(21)	2.843(4)	Ba−O(22)	2.745(4)
Ba−O(31)	2.964(5)	Ba−O(32)	2.887(4)
Ba−O(51)	2.964(5)	Ba−O(52)	2.910(4)
Ba−O(41)	2.940(6)	Ba−O(61)	2.956(5)
Ba−Ow(1)	2.887(5)		
Ni(1)−N(11)	1.834(6)	Ni(2)−N(12)	1.859(6)
Ni(1)−N(21)	1.858(6)	Ni(2)−N(22)	1.848(5)
Ni(1)−O(11)	1.853(4)	Ni(2)−O(12)	1.866(4)
Ni(1)−O(21)	1.849(4)	Ni(2)−O(22)	1.865(4)
O(11)−Ba−O(31)	53.9(1)	O(21)−Ba−O(51)	53.9(1)
O(31)−Ba−O(41)	53.7(1)	O(51)−Ba−O(61)	55.7(1)
O(12)−Ba−O(32)	55.1(1)	O(22)−Ba−O(52)	55.0(1)
C(41)−O(31)−C(81)	116.6(5)	C(42)−O(32)−C(82)	120.3(5)
C(91)−O(41)−C(101)	109.0(7)	C(92)−O(42)−C(102)	111.9(6)
C(141)−O(51)−C(181)	116.8(5)	C(142)−O(52)−C(182)	119.2(4)
C(191)−O(61)−C(201)	111.8(6)	C(192)−O(62)−C(202)	114.6(6)
Ba−O(11)−C(31)	119.9(4)	Ba−O(12)−C(32)	120.5(4)
Ba−O(21)−C(131)	122.2(4)	Ba−O(22)−C(132)	122.0(3)
Ba−O(31)−C(41)	113.9(4)	Ba−O(32)−C(42)	116.1(4)
Ba−O(31)−C(81)	126.8(4)	Ba−O(32)−C(82)	122.4(4)
Ba−O(51)−C(141)	117.7(4)	Ba−O(52)−C(142)	116.1(3)
Ba−O(51)−C(181)	123.6(4)	Ba−O(52)−C(182)	123.1(3)
Ba−O(41)−C(91)	118.8(5)	Ba−O(61)−C(191)	107.5(4)

Within each $(L^2_2Ni)^x$ unit, ($x = 1, 2$) (cf. Figure 2), two deprotonated Schiff base ligands are assembled around the nickel ion in such a way that the resulting NiN$_2$O$_2$ chromophore adopts a cis (or syn) configuration which leads to the formation of an outer site comprising six oxygen atoms. In the $(L^2_2Ni)^1$ unit, the six oxygen atoms are linked to the Ba^{2+} ion, while only four oxygen atoms of $(L^2_2Ni)^2$ participate in the barium coordination sphere. In that instance two methoxy groups of the $(L^2_2Ni)^2$ unit remain free except that they are hydrogen-bonded to the water molecule Ow(1), which completes the coordination sphere of Ba^{2+}. It may be noted that in one of the (L^2_2Ni) units of **4**[9] two methoxy groups are not coordinated to the sodium ion (cf. Figure 1). Coordination of the oxygen atoms to Ba^{2+} leads to the formation of six five-membered chelating rings. Four of them are constrained by the rigidity of the conjugated part of the $(L^2_2Ni)^x$ units to adopt an eclipsed

---

(13) Fair, C. K. *MolEN*: *Molecular Structure Solution Procedures*; Enraf-Nonius, Delft, Holland, 1990.

(14) Sheldrick, G. M. *SHELXS-86*: *Program for Crystal Structure Solution*; University of Göttingen: Göttingen, Germany, 1986.

(15) Sheldrick, G. M. *SHELX76*: *Program for Crystal Structure Determination*; University of Cambridge: Cambridge, England, 1976.

(16) *International Tables for X-Ray Crystallography*; Kynoch Press: Birmingham, England, 1974; Vol. IV.

(17) Johnson, C. K. *ORTEP*; Report ORNL-3794; Oak Ridge National Laboratory: Oak Ridge, TN, 1965.

Table 3. Hydrogen-Bond Lengths (Å) and Angles (deg) for **2**

D	H	A	D−H	H···A	D−H···A	D···A
Ow(1)	Hw(11)	O(62)	0.97(3)	1.89(2)	147(5)	2.753(7)
Ow(1)	Hw(21)	O(42)	0.97(5)	1.84(5)	155(5)	2.751(7)
Ow(2)	Hw(12)	O(71)	0.97(5)	2.29(7)	127(7)	2.981(11)
Ow(2)	Hw(22)	O(72)	0.97(2)	1.80(4)	155(8)	2.714(12)
N(21)	H(N21)	Ow(1′)	0.97	2.13	159	3.057(8)
N(22)	H(N22)	Ow(2)	0.97	2.05	150	2.931(9)

planar conformation (type i) with torsion angles varying from 1.0(9) to 3.3(8)°. The constraint is relieved, at least partially, in the remaining two cycles (type ii), which display the usual gauche conformation with torsion angles of 36.6(9)° [O(31)C(81)C(91)O(41)] and 49.3(9)° [O(51)C(181)C(191)O(61)]. Due to their higher degree of freedom, the monodentate side arms (type iii) display larger torsion angles (58.2(8)° [O(32)C(82)C(92)O(42)] and −65.2(7)° [O(52)C(182)C(192)O(62)]).

It is generally accepted[18−27] that the most important structural requirement for the ideal metal ion−ether donor interaction is attainment of the preferred Ba−O bond length. However, in a recent paper,[27] the importance of the oxygen orientation preference has been emphasized. In complex **2**, the Ba−O distances vary from 2.964(5) to 2.745(4) Å. On the whole, they are consistent with the values (2.87 ± 0.05 Å) observed for other complexes of Ba^{2+} (see ref 27 and references therein). Furthermore they do not significantly differ from the 2.887(5) Å value characterizing the constraint-free Ba−Ow(1) bond. The O−Ba−O angles vary between 53.7(1) and 55.7(1)° and are similar to the values reported in the literature for the ether complexes of barium.[27] All C−O−C angles but three vary between 114.6(6) and 120.3(5)° in accordance with an overall trend toward the desired trigonal planar geometry.[27] This point is supported by the consideration of the Ba−O−C angles, which vary from 116.1(4) to 123.6(4)°, except in two cases where low values (107.5(4) and 113.9(4)°) are observed. The abnormally low values of C−O−C and Ba−O−C are essentially related to oxygen atoms belonging to terminal $-C-O-CH_3$ groups in cycles of type ii and are associated with large values of the C−O bonds. These distortions of bond lengths and angles may be due to steric strain and/or repulsive effects.[28]

The coordination around the nickel ions of the $(L^2{}_2Ni)^x$ ($x = 1, 2$) units is best described as square planar, the four metal donor atoms and the metal being coplanar within ±0.05Å ($x = 1$) and within ±0.005 Å ($x = 2$). The angle between the two mean coordination planes is equal to 165.9(4)° whereas the distances of the barium to these planes are 1.3105(3) and 1.1223(3) Å for the $x = 1$ and 2 units, respectively.

Both ClO_4 anions are hydrogen-bonded to the water molecule Ow(2), the oxygen of which is itself an acceptor for N(22)H. More interestingly the water molecule Ow(1) which is directly bound to Ba^{2+} is also involved in hydrogen bonding with the two "free" OCH_3 groups and the N(21)H group of a symmetry-related ($^1/_2 + x, y, ^3/_2 - z$) unit (Table 3). This results in the formation of a chainlike arrangement of the metallic ions.

Solution Study. The solid state existence and structures of **2**, **3**,[8] and **4**[9] are clearly established by the X-ray diffraction study, but it does not follow necessarily that these species exist unchanged in solution.

From molecular weight determinations [cryoscopy in $(CH_3)_2SO$] and conductance measurements [$(CH_3)_2CO$ and $(CH_3)_2SO$], we may infer that **1**, **3**, and **4** are extensively ionized but the resulting cationic species $[(L^1{}_2Ni)_2Ba]^{2+}$, $[L^1{}_2NiNa]^+$, and $[L^2{}_2NiNa]^+$ remain practically undissociated. In contrast, the data obtained for **2** are far from being consistent with the occurrence of a simple ionization process. Indeed, the ratio of the theoretical to experimental values of the molecular weight, which is expected to give an evaluation of the number of particles present in the solution, has been found equal to 5.8.

For **1**, **3**, and **4**, the ^1H and ^{13}C NMR spectra recorded in $(CH_3)_2CO$ and $(CH_3)_2SO$ are similar, the main differences resulting from a slight dependence of the chemical shifts on the nature of the solvent. In the three cases, the number of signals is consistent with the propounded formulas and the assumption that the two ligands (L^1 or L^2) forming each ($L^i{}_2Ni$) are equivalent. This last point agrees with the known structure of **3** and the likely structure of **1**. However in the case of **4**, ionization is expected to yield two $[L^2{}_2NiNa]^+$ cations which differ by the coordination mode (monodentate vs bidentate) of their $-O-CH_2-CH_2-OCH_3$ side arms. Such a difference would lead to the presence of two sets of CH_2 and CH_3 signals of identical intensity. The observation of one set of resonances even at −80 °C likely results from a rapid exchange process via the sites made vacant by the loss of the anions.

As for complex **2**, in CD_2Cl_2 and $(CD_3)_2SO$, 8 ^1H resonances and 9 ^{13}C resonances are observed, while in $(CD_3)_2CO$, these spectra comprise 12 and 17 signals, respectively. Focusing our attention on the 3.5−4.5 ppm area of the ^1H spectrum (acetone), we observe at room temperature two OCH_3 signals (3.75_8 (a) and 3.72_4 (a′) ppm) and four broad and structureless resonances centered at 4.48_3 (b), 4.26_8 (b′), 4.18_5 (c), and 3.87_9 (c′) ppm respectively (Figure 3). From ^1H COSY and $^1H-^{13}C$ correlation experiments, these features must be attributed to unequivalent $-CH_2-CH_2-OCH_3$ fragments.

Signals a−c are observed from room temperature down to 180 K and their intensity increases on decreasing the temperature. At room temperature, the related δ values are almost identical to those observed for a solution of **2** in CD_2Cl_2. Finally the a−c set may be attributed to the undissociated species $[(L^2{}_2Ni)_2Ba]^{2+}$. As for the second set, the influence of the temperature on the spectral features is larger than in the former case. The intensity of signals a′−c′ decreases on lowering the temperature, and below 193 K the three signals are no longer discernible. At 293 K, the related δ values lie between those of $L^2{}_2Ni$ and those of the 1/1 complex $[L^2{}_2NiBa]^{2+}$, which, most probably, is responsible for the spectrum observed when an excess of Ba^{2+} ions is added to a solution of **2** in acetone. It may be recalled that such a mixture gives a simple ^1H spectrum comprising six signals. Finally the whole body of experimental data is consistent with the following dissociation process:

$$[(L^2{}_2Ni)_2Ba]^{2+} \rightleftarrows [L^2{}_2NiBa]^{2+} + L^2{}_2Ni$$

$$[L^2{}_2NiBa]^{2+} \rightleftarrows L^2{}_2Ni + Ba^{2+}(\text{solvated})$$

A rapid exchange between $L^2{}_2Ni$ and $[L^2{}_2NiBa]^{2+}$ has to be assumed over the 293−193 K temperature range. It may be noted that, below 220 K, signals b′ and c′ give rise to two pairs

---

(18) Christensen, J. J.; Eatough, D. J.; Izatt, R. M. *Chem. Rev.* **1974**, *74*, 351.
(19) Bajaj, A. V.; Poonia, N. S. *Coord. Chem. Rev.* **1988**, *87*, 55.
(20) Vogtle, F.; Weber, E. In *Crown Ethers and Analogues*; Papai, S., Rappaport, Z., Eds.; Wiley: New York, 1989.
(21) Izatt, R. M.; Pawlak, K.; Bradshaw, J. S.; Bruening, R. L. *Chem. Rev.* **1991**, *91*, 1721.
(22) An, H.; Bradshaw, J. S.; Izatt, R. M. *Chem. Rev.* **1992**, *92*, 543.
(23) Lehn, J. M. *Angew. Chem., Int. Ed. Engl.* **1988**, *27*, 89.
(24) Lehn, J. M.; Sauvage, J. P. *J. Am. Chem. Soc.* **1975**, *97*, 6700.
(25) Cram, D. J. *Angew. Chem., Int. Ed. Engl.* **1986**, *25*, 1039.
(26) Cram, D. J. *Science* **1983**, *219*, 1177.
(27) Hay, B. P.; Rustad, J. R. *J. Am. Chem. Soc.* **1994**, *116*, 6316.
(28) Damu, K. V.; Hancock, R. D.; Wade, P. W.; Boyens, J. C. A.; Billing, D. G.; Dobson, S. M. *J. Chem. Soc., Dalton Trans.* **1991**, 293.

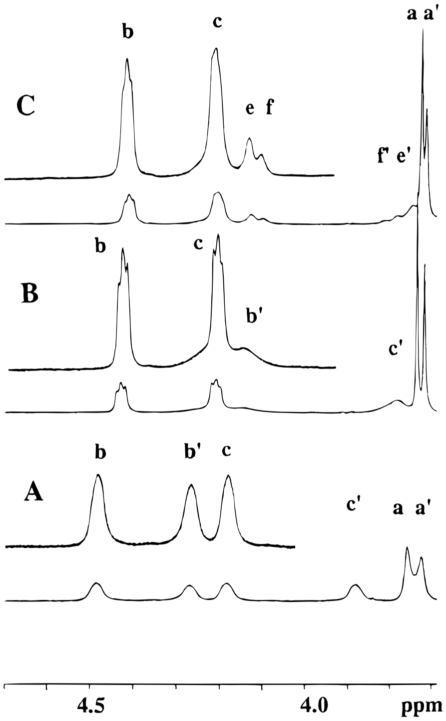

Figure 3. Evolution of the ^{1}H NMR spectra (acetone solution) of **2** with temperature: A, 300 K; B, 233 K; C, 213 K.

of signals e, f and e′, f′. Within each pair the two signals have not the same intensity so that the splitting cannot be caused by a decrease of the rate of the exchange between L^2_2Ni and $[L^2_2NiBa]^{2+}$ but, most probably, is related to the cis–trans conformational equilibrium of the L^2_2Ni species.

As previously noted, the solution of **2** in CD_2Cl_2 and in $(CD_3)_2SO$ gives rise to simple ^{1}H and ^{13}C spectra, each comprising one set of signals. However the δ values notably depend on the nature of the solvent. For CD_2Cl_2 solutions, the CH_2 resonances and the OCH_3 resonance are located at 4.48_3, 4.19_2, and 3.75_9 ppm. These values are strongly reminiscent of those attributed to $[(L^2_2Ni)_2Ba]^{2+}$ in the spectra of **2** in acetone. In the case of $(CD_3)_2SO$ solutions, the δ values do not significantly differ from those observed for L^2_2Ni in the same solvent. From these data, we may infer that **2** is dissociated to a very large extent for $(CD_3)_2SO$ in accordance with the cryoscopic results, while the dissociation is vanishingly small for CD_2Cl_2. This behavior contrasts with that of complexes **1**, **3**, and **4** which remain almost unaffected in CD_2Cl_2, $(CD_3)_2CO$, and $(CD_3)_2SO$.

Acknowledgment. We thank S. Richelme and C. Claparols (Service Commun de Spectroscopie de Masse, Toulouse, France) for their contribution to the mass spectral study and A. Munoz (cryoscopy). The suggestion provided by one of the reviewers, concerning the intervention of $[L^2_2NiBa]^{2+}$ in the dissociation process, is gratefully acknowledged.

Supporting Information Available: A tabular and textual presentation of the experimental X-ray diffraction study and tables of atomic coordinates, thermal parameters, all bond lengths and angles, and least-squares planes calculations for $(L^2_2Ni)_2Ba(ClO_4)_2{\cdot}2H_2O$ (13 pages). Ordering information is given on any current masthead page.

IC960856Y